A Horizontal Wind and Wind Confidence Algorithm for Doppler Wind Profilers

ROBERT K. GOODRICH

National Center for Atmospheric Research, and Department of Mathematics, University of Colorado, Boulder, Colorado*

CORRINNE S. MORSE, LARRY B. CORNMAN, AND STEPHEN A. COHN

National Center for Atmospheric Research, Boulder, Colorado

(Manuscript received 4 April 2000, in final form 11 July 2001)

ABSTRACT

Boundary layer wind profilers are increasingly being used in applications that require high-quality, rapidly updated winds. An example of this type of application is an airport wind hazard warning system. Wind shear can be a hazard to flight operations and is also associated with the production of turbulence. A method for calculating wind and wind shear using a linear wind field assumption is presented. This method, applied to four- or five-beam profilers, allows for the explicit accounting of the measurable shear terms. An error analysis demonstrates why some shears are more readily estimated than others, and the expected magnitudes of the variance for the wind and wind shear estimates are given. A method for computing a quality control index, or confidence, for the calculated wind is also presented. This confidence calculation is based on an assessment of the validity of the assumptions made in the calculations. Confidence values can be used as a quality control metric for the calculated wind and can also be used in generating a confidence-weighted average wind value from the rapid update values. Results are presented that show that errors in the wind estimates are reduced after removing values with low confidence. The wind and confidence methods are implemented in the NCAR Wind and Confidence Algorithm (NWCA), and have been used with the NCAR Improved Moments Algorithm (NIMA) method for calculating moments and associated moment confidence from Doppler spectra. However, NWCA may be used with any moment algorithm that also computes a first moment confidence. For example, a very simple confidence algorithm can be defined in terms of the signal-to-noise ratio.

1. Introduction

The long-term plan in Juneau, Alaska, is to develop a terrain-induced wind shear and turbulence hazard warning system for the airport vicinity. Preliminary research indicates that turbulence in this region, as measured by a research aircraft, is well-correlated with the wind speed and vertical shear of the horizontal wind measured with nearby wind profilers and anemometers. Strong vertical shears of the horizontal wind have been measured near the mountain tops surrounding Juneau and are often associated with strong turbulence. Both the shears and turbulence can be a hazard to aircraft operations. The development of a real-time warning system is the motivation for producing rapid update wind and wind shear estimates from Doppler wind profilers. In most profiler applications, a so-called consensus wind is produced based on measurements over a time period of between 30 and 60 min. Because measurements taken over a fairly long time period are used to compute a consensus wind, spurious outliers in the data can be recognized and removed based on this consensus. However, when a rapid update estimate is required, data quality control becomes a more immediate concern. In a real-time warning system false alarms quickly erode user confidence, so the detection and removal of erroneous data is very important. The National Center for Atmospheric Research (NCAR) Winds and Confidence Algorithm (NWCA) has been developed to provide rapid update estimates of wind and vertical shear of the horizontal wind from wind profiler radial velocities. It also provides an indication of confidence in those estimates. In the case when the confidence in the estimates is low, the wind and shear estimates will not be used in the warning system. NWCA can also produce a confidence-weighted average wind, which may be used for similar applications as traditional consensus winds. The NWCA algorithm has been running at three profiler sites in Juneau, Alaska, since 1998.

To produce these products the wind field is assumed to be horizontally uniform and stationary over the mea-

* The National Center for Atmospheric Research is sponsored by the National Science Foundation.

Corresponding author address: Robert K. Goodrich, National Center for Atmospheric Research, P.O. Box 3000, Boulder, CO 80307-3000.
E-mail: goodrich@ucar.edu

surement volume and duration, while vertical shear of the horizontal wind is allowed. Statistical tests are used to check these assumptions, and when these tests fail a low confidence is given to the wind estimates. Note that failure of these assumptions can be due to atmospheric motions or a result of incorrect moments provided to the algorithm. To test these assumptions, a more general assumption of a stationary, linearly varying wind field is used. This allows for an analysis of biases caused by shears that are not zero, but are set to zero given the horizontally uniform wind field assumption. In Juneau, a four-beam analysis is used, that is, no vertical beam is included in the measurement sequence. In the case of a five-beam system, the assumption of a horizontally uniform wind field can be relaxed to require only that the vertical component of the wind is horizontally uniform. However, it is shown that the additional shear terms (the horizontal shear of the horizontal wind) in this more general wind field are difficult to estimate because they have large variances. In the case of a five-beam system these horizontal shears of the horizontal wind can be estimated by time averaging. With a four-beam system in Juneau, only the vertical shear of the horizontal wind is calculated.

The proposed warning system includes anemometers as well as wind profilers. Because of these additional sensors, the system can continue to function during periods when the assumptions are violated and high-confidence winds are not available at certain heights. This has the effect of reducing false alarms. The warning system is discussed further at the end of section 4.

The assumptions that the wind field is horizontally uniform and stationary are common in wind profiler analysis. For example, estimation of the horizontal wind from radial velocities measured with three-beam wind profilers has been presented by Strauch et al. (1984) and for five-beam wind profilers by Strauch et al. (1987). Koscielny et al. (1984) considered unknown shear terms to be a bias if the wind field is linear rather than horizontally uniform. They applied their work to a three-beam, azimuthal scanning (VAD) and elevation scanning system. There is a long history of the linear wind field assumption for scanning Doppler radars. An early example is the work of Browning and Wexler (1968) where an analysis of the VAD was given in the presence of a linear field, and estimates for mean convergence and shearing deformation were also presented. Waldteufel and Corbin (1979) studied the estimation of various wind field quantities by applying a linear wind field analysis to a volume of radial velocity data (VVP). A more recent example of linear analysis is found in Boccippio (1995), which reviews the VAD and VVP methods using regression diagnostics. All of these analyses assume a linear wind field with additive noise. A regression is performed to estimate some of the linear field parameters by fitting the linear model to measured radial velocity data. In the same spirit, NWCA fits a local linear wind field model to a four- or five-fixed-beam system. Local regressions along fixed beams are used to estimate the horizontal wind and the vertical shear of the horizontal wind field. The appendix further considers these shear terms and effects of noise. A simple mathematical explanation is given for a long observed fact that shears in some directions cannot be individually estimated whereas sums of these shears can be estimated. A confidence index that is used for quality control of the wind estimates has also been developed, based on a variety of tests that determine the suitability of the linearity, spatial homogeneity, and stationarity assumptions.

Although the NWCA algorithm can be used with any moment algorithm that also computes a first moment confidence, it is used in Juneau with the NCAR Improved Moments Algorithm (NIMA; Morse et al. 2002; Cornman et al. 1998). NIMA uses fuzzy logic and global image processing to identify and compute the moments of the atmospheric signal in wind profiler Doppler spectra in the presence of ground clutter, radio frequency interference, and other contamination. A confidence value for the moments is also generated. Using these moments and confidences, the NWCA algorithm then estimates the wind and some components of wind shear from four- or five-beam pointing directions. A study investigating the performance of NIMA and NWCA is described in Cohn et al. (2001), with further results presented in section 6. In this study, human experts identified the atmospheric signal in Doppler spectra, which was then used to compute the first moments, and these first moments were used to compute horizontal wind estimates. These winds were compared to those produced by NWCA. It is shown that for high-confidence winds, there is strong agreement between the human-produced winds and the NWCA-produced winds. This shows the confidence index has skill in identifying high-quality data and in rejecting poor quality data. For a 9-month period, it is estimated that after removing 3% of the data with lowest confidence, the average vector error in the horizontal wind is about 1 m s^{-1}. For the winter period, 18% of the data must be removed to achieve an estimated accuracy of 1 m s^{-1} when compared to a human expert.

2. Calculation of horizontal wind and shear terms from a Doppler wind profiler

Assume that the wind field in a local region above the profiler is well approximated by a linear function. Over a relatively small region of space, a linear model should be a good first-order estimate of the wind field. Furthermore, assume that the wind field is stationary during the time that the profiler cycles through the beam directions. These assumptions are made for the region containing the radial data that are used in making a particular estimate of the horizontal wind. For a four-beam system, this region is in the shape of a frustum of a cone, and the size of this frustum increases with

height. This frustum is described in more detail later in this section. At the top of our analysis cone (2500 m) the horizontal scale is 1.3 km. Based on these assumptions, a method for estimating the linear wind field parameters, including the effect of shears, is presented for the case of no noise. In this case, an algorithm for computing the horizontal wind and shears should return the exact values of some of the linear wind field parameters. In the appendix an error analysis that accounts for measurement noise is given. Persistent vertical shears of the horizontal wind over hundreds of meters can be a hazard to flight. The assumptions that the wind field is linear and stationary are tested using various statistical techniques as shown in section 4. When these tests indicate that the assumptions might not be correct, a low confidence is assigned to the horizontal wind estimates. Low confidence winds and low confidence vertical shears of the horizontal winds will not be used in a warning system to estimate hazards.

Assume a linear wind field of the form,

$$\mathbf{V}(\mathbf{x}) = \mathbf{V}(\mathbf{x}_o) + \mathbf{A} \cdot (\mathbf{x} - \mathbf{x}_o), \tag{1}$$

where $\mathbf{x}$ is a point in space and $\mathbf{x}_o$ is an arbitrary reference point, that is,

$$\mathbf{x} = \begin{bmatrix} x \\ y \\ z \end{bmatrix} \quad \text{and} \quad \mathbf{x}_o = \begin{bmatrix} x_o \\ y_o \\ z_o \end{bmatrix};$$

$\mathbf{V}(\mathbf{x}_o)$ is the velocity at $\mathbf{x}_o$; and $\mathbf{A}$ is a matrix of the wind shears, that is,

$$\mathbf{V}(\mathbf{x}_o) = \begin{bmatrix} u_o \\ v_o \\ z_o \end{bmatrix}, \quad \text{and} \quad \mathbf{A} = \begin{bmatrix} u_x & u_y & u_z \\ v_x & v_y & v_z \\ w_x & w_y & w_z \end{bmatrix},$$

and $\mathbf{A} \cdot (\mathbf{x} - \mathbf{x}_o)$ is the matrix multiplication of $\mathbf{A}$ and the column vector $(\mathbf{x} - \mathbf{x}_o)$. The parameter u_x represents the x direction shear of the wind parallel to the x axis, that is, $u_x = \partial u/\partial x$, v_y represents the y direction shear of wind parallel to the y axis, etc. Note that $\mathbf{A}$ is independent of position since a linear-field approximation is based on constant shears over the local domain. Hence the entries in this matrix can be measured at any point and applied to all others. Likewise, the linear assumption allows any convenient point to be chosen as the reference point $\mathbf{x}_o$. That the choice of reference point is arbitrary is shown in Eq. (2) below by adding and subtracting a constant vector $\mathbf{x}_1$:

$$\begin{aligned} \mathbf{V}(\mathbf{x}) &= \mathbf{V}(\mathbf{x}_o) + \mathbf{A} \cdot (\mathbf{x} - \mathbf{x}_o) \\ &= \mathbf{V}(\mathbf{x}_o) + \mathbf{A} \cdot (\mathbf{x} - \mathbf{x}_1 + \mathbf{x}_1 - \mathbf{x}_o) \\ &= \mathbf{V}(\mathbf{x}_o) + \mathbf{A} \cdot (\mathbf{x}_1 - \mathbf{x}_o) + \mathbf{A} \cdot (\mathbf{x} - \mathbf{x}_1) \\ &= \mathbf{V}(\mathbf{x}_1) + \mathbf{A} \cdot (\mathbf{x} - \mathbf{x}_1), \end{aligned} \tag{2}$$

where $\mathbf{V}(\mathbf{x}_1) = \mathbf{V}(\mathbf{x}_o) + \mathbf{A} \cdot (\mathbf{x}_1 - \mathbf{x}_o)$.

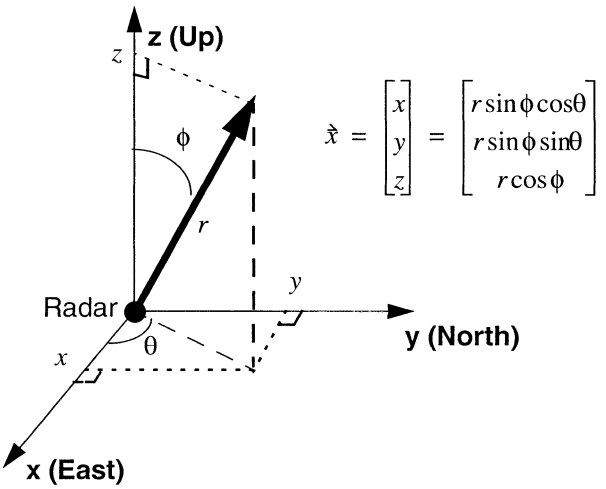

FIG. 1. Wind analysis Cartesian and spherical coordinate system with radar at the origin. The vector $\mathbf{x}$ is expressed in spherical coordinates. The angle ϕ is the angle between the z axis and the vector $\mathbf{x}$. Note that for convenience of the mathematical analysis, a right-handed coordinate system with z positive away from the ground is used and θ being measured counterclockwise from the x axis. This contrasts with the normal meteorological convection of measuring azimuth clockwise from north.

In the analysis of the profiler measurements, it is convenient to use spherical coordinates as shown in Fig. 1, where the radar is at the origin, $x = r \sin\phi \cos\theta$, $y = r \sin\phi \sin\theta$, and $z = r \cos\phi$, where ϕ is the zenith angle, θ is the azimuth measured counterclockwise from the x axis, and r is the length of the vector $\mathbf{x}$.

Consider the velocity vector $\mathbf{V}_V = \mathbf{V}(\mathbf{x}_V) = [u_V, v_V, w_V]^T$ at the point $\mathbf{x}_V(r_o) = [0, 0, z_V]^T = [0, 0, r_o \cos\phi]^T$, which is directly above the radar at the height $z_V = r_o \cos\phi$, where r_o is the distance from the radar to the center of a pulse volume of a nonvertical beam. The height $z_V = r_o \cos\phi$ is used since this is the height at which estimates are given in the nonvertical beams. Here the subscript V refers to the vertical direction. Capital letter subscripts such as E, W, S, and N refer to the directions of east, west, north, and south, respectively. For convenience, these directions are assumed to be aligned with the profiler coordinate system. Thus the direction of E corresponds to the positive x axis and N corresponds to the positive y axis, etc. This is done only to facilitate the discussion since it is a simple task to express the horizontal wind vector in terms of any other orthogonal coordinate system, that is, performing a rotation.

The goal of this analysis is to estimate the horizontal component of the wind vector at the point directly above the profiler. As will be shown below, for a four-beam system and the assumption of a linear wind field, this is the only point at which the horizontal velocity component can be estimated. This is due to the fact that shears of the horizontal wind component cannot be estimated. For a five-beam system, these shears can be estimated, however, in general, regardless of the number

of beams, the horizontal shears of the vertical component cannot be estimated without additional assumptions. Starting with data from an oblique profiler beam, for example, the east beam, such that $\phi \neq 0$ and $\theta = 0$, consider the point $\mathbf{x}_E(r_o) = [r_o \sin\phi, 0, r_o \cos\phi]^T$. The vector velocity at this point is $\mathbf{V}[\mathbf{x}_E(r_o)]$. Assuming that the profiler returns an unbiased estimate of the radial velocity at $\mathbf{x}_E$, the radial velocity at that point is denoted by $V(\mathbf{x}_E)$. Thus the radial velocity field is a measured quantity from the profiler. Note that the radial velocity along the east beam is defined as the inner product of the wind vector with the unit vector along the radial, $V_E(r) = \mathbf{V}[\mathbf{x}_E(r)] \cdot \mathbf{e}_E$, where r is a location along the radial and $\mathbf{e}_E = \mathbf{x}_E/\|\mathbf{x}_E\| = [\sin\phi, 0, \cos\phi]^T$, where $\|\mathbf{x}\|$ is the length of vector $\mathbf{x}$.

Consider the variation of the wind along the east beam. Using a linear field expansion around the point $\mathbf{x}_E(r_o)$ [Eq. (1)] and along the radial, that is, where the set of points is restricted to vectors of the form $\mathbf{x} = [r \sin\phi, 0, r \cos\phi]^T$, and assuming the vector wind at $\mathbf{x}_E(r_o)$ is $\mathbf{V}[\mathbf{x}_E(r_o)] = [u_E, v_E, w_E]^T$ yields

$$\begin{aligned} V_E(r) &= u_E \sin\phi + u_x(r - r_o)\sin^2\phi \\ &\quad + u_z(r - r_o)\cos\phi\sin\phi + w_E\cos\phi \\ &\quad + w_x(r - r_o)\sin\phi\cos\phi + w_z(r - r_o)\cos^2\phi \\ &= (u_E\sin\phi + w_E\cos\phi) \\ &\quad + [u_x\sin^2\phi + (u_z + w_x)\cos\phi\sin\phi \\ &\quad\quad + w_z\cos^2\phi](r - r_o) \\ &= a_E + b_E(r - r_o). \end{aligned} \tag{3}$$

The constants a_E and b_E may be determined by application of the singular value decomposition (SVD) method to solve a linear least squares fit to the data (see Forsythe et al. 1977, p. 192). These values are estimated quantities. Data from the few nearest range gates $r = r_o \pm i\Delta r$ are used; that is, the linear model in Eq. (3) is fit to the measured radial velocity data at $V_E(r_o \pm i\Delta r)$. In a typical application, i varies from 0 to 2 for a range gate size Δr of 60 m. The maximum value of i is limited to ensure that the linear model is valid and in order to detect shears on a scale of interest to aircraft response. Confidence in the radial first moments is available from NIMA and the fit is weighted by these confidence values. In general, the confidence-weighted average of the first moments used in the linear fit will be the same as the confidence-weighted average of the linear model. When the confidences are all equal, a_E will be the average of the first moments used in the linear fit. In the absence of noise, the coefficients a_E and b_E are determined exactly in the local linear wind field model. Thus,

$$\begin{aligned} a_E &= u_E\sin\phi + w_E\cos\phi \\ b_E &= u_x\sin^2\phi + (u_z + w_z)\cos\phi\sin\phi + w_z\cos^2\phi. \end{aligned} \tag{4}$$

Using data from the opposite west beam (i.e., $\phi \neq 0$, $\theta = 180°$, $\cos\theta = -1$) and expanding about a point at the same range, r_o, $\mathbf{x}_W(r_o) = [-r_o\sin\phi, 0, r_o\cos\phi]^T$, the radial velocity is expressed by $V_W(r_o) = \mathbf{V}[\mathbf{x}_W(r_o)] \cdot \mathbf{e}_W$, with $\mathbf{e}_W = [-\sin\phi, 0, \cos\phi]^T$.

Applying Eq. (1) at the points $\mathbf{x}(r) = [-r\sin\phi, 0, r\cos\phi]^T$ again in the direction of the radial, and assuming the vector wind at $\mathbf{x}_W(r_o)$ is $\mathbf{V}[\mathbf{x}_W(r_o)] = [u_W, v_W, w_W]^T$ yields

$$\begin{aligned} V_W(r) &= -u_W\sin\phi + u_x(r - r_o)\sin^2\phi \\ &\quad - u_z(r - r_o)\cos\phi\sin\phi + w_W\cos\phi \\ &\quad - w_x(r - r_o)\sin\phi\cos\phi + w_z(r - r_o)\cos^2\phi \\ &= (-u_W\sin\phi + w_W\cos\phi) \\ &\quad + [u_x\sin^2\phi - (u_z + w_x)\cos\phi\sin\phi \\ &\quad\quad + w_z\cos^2\phi](r - r_o) \\ &= a_W + b_W(r - r_o), \end{aligned} \tag{5}$$

where a_W and b_W are again determined by application of the SVD method. Again in the absence of noise,

$$\begin{aligned} a_W &= -u_W\sin\phi + w_W\cos\phi \\ b_W &= u_x\sin^2\phi - (u_z + w_x)\cos\phi\sin\phi + w_z\cos^2\phi. \end{aligned} \tag{6}$$

Note that the shear values from the matrix $\mathbf{A}$ are the same at $\mathbf{x}_W$ as they are at $\mathbf{x}_E$ and so the terms from opposite beams may be combined. The difference of the a terms in Eqs. (4) and (6) yields

$$a_E - a_W = (u_E + u_W)\sin\phi + (w_E - w_W)\cos\phi. \tag{7}$$

To determine the values of u_E, u_W, w_E, and w_W, Eq. (1) is applied to determine the wind directly over the profiler, at the point, $\mathbf{x}_V(r_o) = [0, 0, r_o\cos\phi]^T$. First from the east beam:

$$\begin{aligned} \begin{bmatrix} u_V \\ v_V \\ w_V \end{bmatrix} &= \mathbf{V}(\mathbf{x}_V(r_o)) \\ &= \mathbf{V}(\mathbf{x}_E(r_o)) + \mathbf{A}\cdot(\mathbf{x}_V(r_o) - \mathbf{x}_E(r_o)) \\ &= \begin{bmatrix} u_E - u_x r_o\sin\phi \\ v_E - v_x r_o\sin\phi \\ w_E - w_x r_o\sin\phi \end{bmatrix} \end{aligned} \tag{8}$$

and from the west beam:

$$\begin{aligned} \begin{bmatrix} u_V \\ v_V \\ w_V \end{bmatrix} &= \mathbf{V}(x_W(r_o)) \\ &= \mathbf{V}(\mathbf{x}_V(r_o)) + \mathbf{A}\cdot(\mathbf{x}_V(r_o) - \mathbf{x}_W(r_o)) \\ &= \begin{bmatrix} u_W + u_x r_o\sin\phi \\ v_W + v_x r_o\sin\phi \\ w_W + w_x r_o\sin\phi \end{bmatrix}. \end{aligned} \tag{9}$$

Adding Eqs. (8) and (9) yields

$$u_E + u_W = 2u_V \qquad v_E + v_W = 2v_V$$
$$w_E + w_W = 2w_V, \tag{10}$$

and subtracting them yields

$$u_E - u_W = 2u_x r_o \sin\phi \qquad v_E - v_W = 2v_x r_o \sin\phi$$
$$w_E - w_W = 2w_x r_o \sin\phi. \tag{11}$$

Now it is necessary to assume $w_x = 0$ so that $w_E = w_W$. Subsequently, when considering the N–S beams, a similar condition for w_y will be imposed. The assumption that $w_x = w_y = 0$ implies that the vertical component of the wind field is locally homogenous. This is a common assumption in profiler wind measurements, although it may be violated, for example, in a terrain-induced (stationary) gravity wave. If this assumption is violated there will be an error in the wind calculation. In this case, the wind estimates will be biased as shown in Eq. (A7) in the appendix. This is similar to a result found in Koscielny et al. (1984). In section 3 it is shown that in the case of a linear wind field, the terms w_x and w_y cannot be determined without additional assumptions. An indirect test for the assumption that the vertical component of the wind is horizontally uniform is discussed in section 4. In most cases, the system should assign low confidence to such estimates when this assumption is violated.

With the assumption that $w_x = 0$, Eqs. (7) and (10) can be combined to find the component of the horizontal velocity along the E–W axis at the point $(0, 0, z_V)$:

$$u_V = \frac{a_E - a_W}{2 \sin\phi}. \tag{12}$$

Note that no derivative assumptions are required beyond the assumption that $w_x = 0$. Note that since the linear field is expanded around $(0, 0, z_V)$, the effect of the u_x shear is zero. By similar reasoning (and assuming $w_y = 0$), an estimate for the component of the horizontal velocity along the N–S axis at the point $(0, 0, z_V)$ is given by

$$v_V = \frac{a_N - a_S}{2 \sin\phi}. \tag{13}$$

An estimate of the vertical component of the wind from the oblique beams is also possible. Adding a_E and a_W from Eqs. (4) and (6) gives the following result:

$$a_E + a_W = (w_E + w_W)\cos\phi + (u_E - u_W)\sin\phi. \tag{14}$$

Substituting from Eqs. (10) and (11), produces

$$a_E + a_W = 2w_V \cos\phi + 2u_x r_o \sin^2\phi. \tag{15}$$

The estimate for the vertical component of the wind at the point $(0, 0, z_V)$ is thus

$$w_V = \frac{(a_E + a_W) - 2u_x r_o \sin^2\phi}{2 \cos\phi}. \tag{16}$$

The vertical wind can also be estimated using the north and south beams

$$w_V = \frac{(a_N + a_S) - 2v_y r_o \sin^2\phi}{2 \cos\phi}. \tag{17}$$

Consider an estimate of the term $(u_x r_o \sin^2\phi)/(\cos\phi)$. If $u_x = 0.01\ \text{s}^{-1}$, which is a fairly large horizontal shear, $\phi = 15°$ (typical for wind profilers), and $r_o = 2500$ m, then $(u_x r_o \sin^2\phi)/(\cos\phi) = 1.73\ \text{m s}^{-1}$. This is a significant error. If a horizontally uniform wind field is assumed, instead of a general linear field, the shear terms would vanish and the two vertical estimates would be

$$w_V = \frac{a_E + a_W}{2 \cos\phi} \tag{18}$$

$$w_V = \frac{a_N + a_S}{2 \cos\phi}. \tag{19}$$

In section 3, it will be shown that it is possible to measure u_x if a vertical beam is available, that is, in a five-beam system. However, for a wind profiler operating without a vertical beam, as is the case in the current Juneau operations, Eqs. (18) and (19) must be used. This requires the assumption of a horizontally uniform wind field. The variances for these estimates in the presence of noise are discussed in the appendix. Equations (18) and (19) are used in section 4 to test the assumption of a horizontally uniform wind field.

3. Closer examination of the shear terms

Using Eqs. (4) and (6) and their analogs for the north and south beams it is possible to give estimates for some shear terms:

$$u_x = \frac{b_E + b_W}{2 \sin^2\phi} - w_z \frac{\cos^2\phi}{\sin^2\phi}$$
$$v_y = \frac{b_N + b_S}{2 \sin^2\phi} - w_z \frac{\cos^2\phi}{\sin^2\phi}$$
$$u_z + w_x = \frac{b_E - b_W}{2 \cos\phi \sin\phi}$$
$$v_z + w_y = \frac{b_N - b_S}{2 \cos\phi \sin\phi}. \tag{20}$$

If a vertical beam is available, w_z can be directly estimated and it is possible to give an estimate of u_x. If an additional azimuth such as $\theta = 45°$ were available, the quantity $v_x + u_y$ could be estimated as well.

To further understand the limitations of estimating shears reconsider Eq. (1). The radial velocity along a general direction $\mathbf{e}$ is given by $V_r = \mathbf{V}(\mathbf{x}) \cdot \mathbf{e} = \mathbf{V}(\mathbf{x}_o) \cdot \mathbf{e} + \mathbf{A} \cdot (\mathbf{x} - \mathbf{x}_o) \cdot \mathbf{e}$, where $\mathbf{e} = \mathbf{x}/\|\mathbf{x}\| = [\sin\phi \cos\theta, \sin\phi \sin\theta, \cos\phi]^T$. In considering only the radial component of the wind seen by a single beam, $\mathbf{x}$ and $\mathbf{x}_o$ are restricted to be along the radial, $\mathbf{x} = r\mathbf{e}$ and $\mathbf{x}_o = r_o\mathbf{e}$ so that $\mathbf{x} - \mathbf{x}_o = (r - r_o)\mathbf{e}$, where r and r_o are the distances of the points $\mathbf{x}$ and $\mathbf{x}_o$, respectively, from the profiler. Then

$$\mathbf{A}\cdot(\mathbf{x}-\mathbf{x}_o)\cdot\mathbf{e} = (r-r_o)\left(\frac{\mathbf{A}+\mathbf{A}^{\mathrm{T}}}{2}\right)\cdot\mathbf{e}\cdot\mathbf{e} + (r-r_o)\left(\frac{\mathbf{A}-\mathbf{A}^{\mathrm{T}}}{2}\right)\cdot\mathbf{e}\cdot\mathbf{e} = \left(\frac{\mathbf{A}+\mathbf{A}^{\mathrm{T}}}{2}\right)(r-r_o)\cdot\mathbf{e}\cdot\mathbf{e}. \quad (21)$$

The second term on the right-hand side of Eq. (21) vanishes because $\mathbf{A} - \mathbf{A}^{\mathrm{T}}$ is antisymmetric; that is, $(\mathbf{A} - \mathbf{A}^{\mathrm{T}})^{\mathrm{T}} = \mathbf{A}^{\mathrm{T}} - \mathbf{A} = -(\mathbf{A} - \mathbf{A}^{\mathrm{T}})$, where $\mathbf{A}^{\mathrm{T}}$ is the transpose of $\mathbf{A}$. This can be shown by considering any antisymmetric matrix $\mathbf{M}$, that is, a matrix for which $\mathbf{M}^{\mathrm{T}} = -\mathbf{M}$. The identity $(\mathbf{My})\cdot\mathbf{y} = \mathbf{y}\cdot(\mathbf{M}^{\mathrm{T}}\mathbf{y}) = \mathbf{y}\cdot(-\mathbf{My}) = -(\mathbf{My}\cdot\mathbf{y})$ can only be true if $\mathbf{My}\cdot\mathbf{y} = 0$. Thus the only measurable terms in Eq. (21) are the shears in $(\mathbf{A} + \mathbf{A}^{\mathrm{T}})/2$ (the symmetric part of $\mathbf{A}$):

$$\frac{\mathbf{A}+\mathbf{A}^{\mathrm{T}}}{2} = \begin{bmatrix} u_x & \dfrac{u_y+v_x}{2} & \dfrac{u_z+w_x}{2} \\ \dfrac{v_x+u_y}{2} & v_y & \dfrac{v_z+w_y}{2} \\ \dfrac{w_x+u_z}{2} & \dfrac{w_y+v_z}{2} & w_z \end{bmatrix}. \quad (22)$$

These are the shears shown in Eq. (20) and the additional shear term $v_x + u_y$, which may be found with an additional beam azimuth such as $\theta = 45°$. Thus a profiler cannot measure u_z, v_z, w_x, or w_y directly but it can measure $u_z + w_x$ and $v_z + w_y$. If u_z is replaced by $u_z + c$ and w_x is replaced by $w_x - c$, where c is an arbitrary constant, then the radial velocity field given in Eq. (21) will not change. This shows that for a linear wind field, it is impossible to measure w_x and w_y directly without further assumptions. So in order to estimate u_z and v_z, it must be assumed that w_x and w_y (the horizontal shears of the vertical component of the wind) are zero or at least small. This is equivalent to assuming that the vertical component of the wind is constant in a horizontal plane, an assumption that could fail with a complicated wind field, such as that near significant terrain. Section 4 discusses an indirect test for this assumption. Shear estimates are typically quite noisy and hence these estimates must be averaged over time and/or space. The space averaging is accomplished by the linear fit, Eq. (A6). The shear estimates are noisy because $\sin\phi$ is quite small for small angles ϕ and $\sin\phi$ appears in the denominator in Eq. (20), magnifying the error in the case of noise. Estimates for the vertical shears of the horizontal component of the wind, u_z and v_z, are often found by direct computation from averaged measurements of u and v over range gates along a beam. In the case when the wind field is linear these average wind shears are approximations to $u_z + w_x$ and $v_z + w_y$. The shear of the horizontal wind field is defined to be the length of the vector difference of the horizontal winds at two different heights above the profiler divided by the change in height. In the case of a linear wind field, this equals $(u_z^2 + v_z^2)^{1/2}$. In order to estimate this shear in the vertical wind, the assumption that the vertical wind is horizontally uniform is required, that is, $w_x = w_y = 0$. See appendix for an analysis of the shear terms u_x and u_z.

It is possible to use this analysis to construct two linear wind fields with the property that they both have the same radial velocity field, but the horizontal winds above the profiler are not equal. This is done by rewriting the wind field in Eq. (2) as:

$$\mathbf{V}(\mathbf{x}) = [\mathbf{V}(\mathbf{x}_o) - \mathbf{A}\cdot\mathbf{x}_o] + \mathbf{A}\cdot\mathbf{x}.$$

Now change the matrix $\mathbf{A}$ to a matrix $\mathbf{A}'$; that is, replace u_z in $\mathbf{A}$ with $u_z + c$ in $\mathbf{A}'$, where c is some constant. Also, replace w_x in $\mathbf{A}$ by $w_x - c$ in $\mathbf{A}'$. The new linear wind field is then given by

$$\mathbf{V}'(\mathbf{x}) = [\mathbf{V}(\mathbf{x}_o) - \mathbf{A}\cdot\mathbf{x}_o] + \mathbf{A}'\cdot\mathbf{x}.$$

It is easy to see that these two wind fields will have the same radial wind values at all points and all beams. It is also easy to see that horizontal wind fields do not agree at x_0 where x_0 is on the z axis. See the discussion before Eq. (22). It is not likely that this exact set of circumstances could occur in real data, but it does point out the possibility that two radial wind fields could look very much alike, but the horizontal winds would not agree. This occurs in the case of large horizontal shears in the vertical wind or in the case of large temporal changes of the vertical wind. These horizontal shears of the vertical wind cause a bias in the estimates for the horizontal winds [Eq. (A7)], and are a fundamental limitation of wind profiler geometry. Thus it is important to detect such situations, and give such winds low confidence. This is discussed is section 4, where benefits of incorporating a vertical beam are also discussed.

4. The horizontal wind confidence estimate

From an operational point of view, it is important to give a confidence estimate for each horizontal wind estimate. For example, if the winds are used to detect an apparent operational hazard, data may not be used if the wind confidence is low. Cohn et al. (2001) demonstrate that the current wind confidence algorithm does have skill in predicting the similarity of NWCA winds to those considered to be truth by an expert. Based on this study some performance results are given in section 6. Cohn et al. (2001) also give a comparison to aircraft wind measurements.

The confidence estimates are produced using fuzzy logic methods. See Cornman et al. (1998) and Morse et al. (2002) for a more complete description of fuzzy algorithms applied to profilers. A human expert might determine the wind confidence based on assessing the

validity of the assumptions that were used to calculate the winds. These assumptions are that

1) the radial velocity moments used in the SVD determination of a and b were correct;
2) the local linear wind model is a good model of the atmosphere;
3) the vertical wind has no horizontal shear, that is, $w_N = w_S = w_E = w_W$, $w_x = w_y = 0$, and $u_x = u_y = 0$ in the case of a four-beam analysis; and
4) the atmosphere is relatively stationary in time and space over the period when the various radar beams were collected.

The fuzzy logic method attempts to replicate the procedure of the human expert. A confidence value for each of these assumptions can be estimated and then geometrically combined using fuzzy logic to produce a final confidence for each of the wind components,

$$C = \left(\prod_{i=1}^{4} c_i^{d_i} \right)^{1/\Sigma_i d_i}, \tag{23}$$

where C is the final confidence, c_i are the individual confidence factors chosen such that $0 \leq c_i \leq 1$ for each i, and d_i are the weights of the individual factors. The combined confidence C has the property that if each confidence value is the same then the combined confidence will equal this common value. In addition, a zero or small confidence in one value makes the combined confidence zero or small. This technique requires each confidence to be close to 1 in order that the combined confidence be close to 1. The weights d_i could be chosen from analyzing data to determine which confidence indices best predict overall confidence. In the present algorithm, each $d_i = 1$.

Confidence estimates are calculated separately for each of the horizontal wind components, that is, C_u and C_v for the u and v, respectively. These are based on four individual confidence factors, described below. First consider the confidence estimate, C_u, for u, the x component of velocity. The confidence c_1 is determined by the average of the confidences associated with each Doppler first moment used to produce the a values at a given height [see Eqs. (4) and (6), and the remarks before Eq. (4)]. These first moment confidences are determined based on such factors as the Gaussian fit to the spectral signal, the signal-to-noise ratio, and the continuity of the first moments as a function of range, as described by Morse et al. (2002).

In section 2 it was assumed that the wind could be modeled with a linear field. This implies that the radial velocity may also be modeled with a linear field. Confidence c_2 is based on how well the data fits the linear model, for example, $V_i = a + b(r_i - r_o)$, and is based on a chi-square test of this assumption:

$$\chi^2 = \sum_{i=-K}^{K} \frac{\langle V_i - [a + b(r_i - r_o)] \rangle^2}{\sigma_i^2}, \tag{24}$$

where σ_i^2 is the variance of the first moment data. For a given first moment estimate, the variance of the estimate is unknown. However, as this first moment is calculated by averaging a number of spectra as a function of time, for example, 50 or so samples over a 30 s dwell interval, the variation of these ''raw'' first moments over the dwell time is reflected in the Doppler second moment. Therefore the second moment is used as surrogate for the true variance of the first moments. The offset of the range gate from the center range gate at r_o is given as $i\Delta r$. For a discussion of the chi-square test see Freund (1992, pp. 309 and 512). In order to compare the fuzzy algorithm for computing c_2 to a statistical analysis, it is assumed that the variances are all nearly equal and this allows for estimating σ_i^2 as the average of the σ_i^2 over the several range gates. It is assumed that σ_i^2 is very close to the actual variance as the spectra contain a large number of sampled points.

The theory for the chi-square test makes several statistical assumptions that are often violated in practice. The standard chi-square test assumes the data are given by a linear model plus Gaussian noise and σ^2 is the variance of the Gaussian process. The coefficients a and b are estimated via the SVD method, which minimizes a residual [given by Eq. (A4)]. In order to connect these two methods, the σ_i^2 and the c_i in Eq. (A4) are assumed to be nearly constant. Then the estimates for a and b from each of these methods are nearly the same. Also the chi-square test assumes the data samples are independent with a normal distribution, while the first moment data could be dependent and the errors do not always have a normal distribution. However, it can be seen that the larger χ^2 is, the less likely it is that the computed linear model is a good fit to the data. This chi-square test compares well to a statistical analysis when the errors in the Doppler first moments are Gaussian and the confidences are all nearly equal, thus matching the equal-weight assumption implied by using the average σ_i^2 in Eq. (24).

A method for converting this χ^2 value into a confidence index between 0 and 1 is required. A reasonable choice for this method is the probability, $Q\langle \chi^2 \mid \nu \rangle$, that χ^2 is greater than or equal to χ^2 if the model is correct. The number of degrees of freedom ν is one less than the number of points used in the fit minus the number of independent parameters replaced by estimates. In the current application, the number of points is $2K + 1$, the number of parameters estimated is 2, a and b for the linear field, for a resulting $\nu = 2K - 2$. The probability Q is calculated using the incomplete Gamma function using a routine in *Numerical Recipes in C* (Press et al. 1988, see formula 6.2.18 p. 177). The confidence based on how well the data fit a linear model is just this probability Q, but the fuzzy methodology allows for scaling this value if need be. Thus this ''chi-square'' test should be viewed strictly as an input to a fuzzy algorithm, which is motivated by statistics, and not as a rigorous

statistical test. As in all fuzzy algorithms, the final test is performance (see section 6).

The assumptions that $u_x = v_y = 0$ (in the four-beam analysis) require testing. There is no direct test for the assumption that $w_x = w_y = 0$ [see the discussion directly following Eq. (20)]. However, the assumption $u_x = v_y = 0$ implies that the two estimates for the vertical component of the wind given by Eqs. (18) and (19) are equal when there is no noise. This implies that, assuming local stationarity in the wind, a time series of estimated vertical components of the wind using alternate north–south and east–west beams should be nearly constant. If $w_x = w_y = 0$, the estimates of the vertical wind component should also be constant as the wind field advects past the profiler over time. Thus to indirectly test the assumptions that $u_x = v_y = w_x = w_y = 0$, a confidence index c_3 should be defined to test the condition that the time series of the estimates of the vertical components of the wind is nearly constant.

In fact, estimation of the confidence c_3 is itself a fuzzy module with three factors and is calculated analogously to the confidence in Eq. (23). The factors include a test of the temporal stationarity and spatial homogeneity of the vertical component of the wind (estimated from all beam directions), whether the current estimate of the vertical component is consistent with a prediction based on the time series, and finally the variance of the estimates in the time series.

To make these tests, a Least Square Adaptive Polynomial [LSAP, also called discounted least squares, see Abraham and Ledolter (1983, p. 101)] fit to the derived time series of vertical components of the wind as calculated by Eqs. (18) and (19), is used. The temporal stationarity and spatial homogeneity can be estimated based on the value of the first-order coefficient of the quadratic polynomial fit. If this value is small then the vertical winds are relatively constant. This coefficient value is mapped into a confidence value such that when the coefficient is large the confidence is low and when the coefficient is small the confidence is high. The next criterion is whether the particular vertical component of the wind calculated from the current beam set w_{obs} is a good fit within the LSAP model w_{pred}, where w_{pred} is the predicted value from the time series fit. An outlier value for the vertical component should result in a low confidence in the associated horizontal wind component. A test that performs this function utilizes the Z statistic,

$$Z = \left[\frac{(w_{\text{obs}} - w_{\text{pred}})^2}{\sigma^2_{\text{pred}}}\right]^{1/2}, \tag{25}$$

where σ^2_{pred} is the variance estimate produced by the LSAP algorithm. A small Z value gives a high confidence and a large Z value gives a low confidence. However, a small Z value could also result if σ^2_{pred} is large, so this variance is checked as the final criterion. If the variance of the prediction is large, there is less confidence in the ability of the LSAP to predict the vertical wind and consequently less confidence in its temporal stationarity.

The final criterion c_4 for the confidence in the u wind component is based on applying an LSAP model to the time series of u wind components and assessing the Z statistic calculated analogously to Eq. (25).

The confidences c_1, c_2, c_3, and c_4 are combined by Eq. 23 to give C_u. Note that if any input to the confidence is zero, the final confidence will also be zero. A similar analysis is performed to calculate C_v, the confidence in the v wind component. The overall confidence in the horizontal wind speed is calculated using the confidence in the u and v wind components; that is, $C = \sqrt{(C_u^2 + C_v^2)/2}$.

In a five-beam case (includes a vertical beam) refinements to the system could be made. A rapid temporal change in the measured vertical wind would be an indicator that the time stationarity assumption has failed. This would lower the confidence in the horizontal wind estimates, but this rapid variation of the vertical wind could be used as a regressor for turbulence. A large vertical variation in the vertical wind would (by mass continuity) indicate a large two-dimensional divergence or convergence in the horizontal wind near the profiler (horizontal shear). The horizontal shears of the horizontal winds could also be estimated. These estimates have a large variance, but they could be time averaged. Such persistent shears could be used as a regressor to estimate turbulence. These matters are under study.

In addition to testing assumptions of the wind field, a practical application of the NWCA confidence algorithm is removal of outlier radial velocities. NIMA removes many outliers from the first moment estimates, but it does not remove all outliers (see Cohn et al. 2001). Winds produced from first moment data containing outliers usually do not satisfy all of the wind tests and usually (but not always) have a low NWCA confidence. If the measurement errors in a_E, a_W, a_N, and a_S are, respectively, e_E, e_W, e_N, and e_S, then from Eqs. (18) and (19) the two estimates of the vertical wind will be the same only if $e_E + e_W = e_S + e_N$.

It follows that if one beam has a large measurement error and the other beams have small measurements errors, then the vertical wind estimates will not agree. This should result in a low confidence because the time series of the vertical wind will not be nearly constant. This will be true even if a single beam error persists over time, since the times series of the vertical winds alternate between north–south and east–west estimates. A large error in one beam will show up as a choppy vertical component as these estimates alternate. This is a case where the horizontal component of the wind field would be nearly constant over time. This component would be in error, but the NWCA wind confidence would be low. A persistent error such as this can occur if the moment finding algorithm selects a persistent signal such as radio frequency interference (RFI) instead of the atmospheric signal. This can occur in a peak

finding algorithm. NIMA rarely selects RFI, but in weak atmospheric signal cases NIMA may select a nonatmospheric signal, and in rare cases this error can persist in time. If the errors satisfy $e_E + e_W = e_S + e_N$, and this holds over time, then the NWCA confidence would be high. This is not likely in the case of outliers, but it can occur. Isolated errors in a beam will be detected when the linear fit test along the beam fails. NIMA usually selects continuous moments in range, but a peak finding algorithm may select point targets that show up as isolated outliers in the first moments. In order for an outlier wind to be assigned a high confidence, the outlier error in the first moment must persist over space and time, and occur in more than one beam and the errors must satisfy $e_E + e_W = e_S + e_N$ in time as well, an unlikely occurrence. For these reasons, the wind confidence algorithm correctly assigns a low confidence to most wind outliers caused by first moment outlier errors.

The warning system in Juneau will include a system of anemometers and three profilers. An anemometer is collocated with each profiler and pairs of anemometers are located on several nearby peaks. The profilers are located near arrival and departure flight tracks where the aircraft are changing altitude. See Cohn et al. (2001) for a map of the area showing the location of these sensors and the flight tracks. On several of these flight tracks the aircraft is making a sharp turn. A large vertical shear of the horizontal wind over hundreds of meters could be a significant hazard to flight. High-confidence large vertical shears of the horizontal wind have been detected in Juneau. Smaller-scale shears are classified as turbulence. The warning system uses various combinations of regressors to estimate turbulence intensity. Among these are wind speed estimates from the three profilers and vertical shear of the horizontal wind at various heights. In preliminary studies, these quantities add skill to the system when high-confidence data is used. Other regressors are second moment (spectrum width) data from the profilers and anemometers and wind speed estimates from the anemometers. Vertical shear of the horizontal wind may also be estimated from the anemometers at the peak top and the anemometer at the runway. These estimates give no indication of the height of the strongest part of the shear. Each of these regressors have data quality control problems. Because so many combinations of regressors are available, it is possible to use only high-confidence regressors. Using a large number of regressors also allows for the possibility of detecting or mitigating the occasional outlier incorrectly assigned high confidence. In the rare event that there were only a small number of high confidence regressors available, a warning would be sent that the system was impaired. Using a subset of a large number of regressors has the effect of removing false alarms while still allowing for detection using high confidence data.

5. Confidence-weighted average winds

The wind confidence calculated for wind estimates also provides for an alternate computation of the consensus winds, which are the typical output of wind profiler applications. This has the advantage of producing an overall confidence value for the resulting winds. A confidence-weighted average of the wind component values is computed over the selected averaging interval via Eq. (26). The confidence in this average wind value is the average of the confidences in the individual wind values:

$$u_A = \frac{\sum_i C_{u_i} u_{V_i}}{\sum_i C_{u_i}}, \qquad C_{u_A} = \frac{\left(\sum_{i=1}^{n} C_{u_i}\right)}{n}, \tag{26}$$

where u_A is the confidence-weighted average value for the u wind component C_{u_A} is the confidence in u_A, the u_{V_i} are the n wind components calculated [Eq. (12)] from consecutive sets of east and west beams collected during the averaging interval, and the C_{u_i} are the confidences in these u_{V_i} values as calculated by Eq. (23). A similar calculation is performed for the v wind component. When reporting winds as wind speed and direction, the confidence is reported as $\sqrt{(C_{u_A}^2 + C_{v_A}^2)/2}$.

Currently the operational system in Juneau reports 10-min confidence-weighted average wind values calculated in this manner. Winds with confidence values less than 0.5 are reported as ''not available.''

6. Some wind confidence performance results

A confidence algorithm may be used to reduce false alarms in a warning system. In order to make use of a confidence algorithm in this way, it is necessary to quantify the relationship between confidence and measurement errors. Wind estimates should be of high quality when the wind confidence is high. To test this assumption, a dataset was used from an intensive data collection effort in Juneau, Alaska, during February–April in 1998. Three 915-MHz boundary layer profilers were employed in this experiment and are still operational in Juneau. Operational parameters included a pulse repetition frequency of 34 500 s^{-1}, a pulse width of 400 ns, and a dwell time of 30 s. The profilers were located near precipitous terrain and aircraft flight tracks to be able to measure the disturbed winds and turbulence generated by the terrain. The weather conditions in Juneau during this time period ranged from strong frontal passages with significant embedded precipitation (rain, snow, and rain–snow mixture), to strong winds associated with clear-air downslope winds off the Taku Glacier (so-called Taku winds). This combination of weather extremes and nearby terrain made for very challenging conditions for profiler operation. The dataset included a limited number of cases when

a research aircraft was flying near the profilers and the aircraft was providing wind and turbulence estimates. Around 174 profiles (of 36 range gates) were selected for human verification. Most of these profiles in the database were selected to coincide with times when the aircraft was flying near one of the three profilers. The database had Radio Frequency Interference, ground clutter, point targets, and low signal-to-noise cases (SNR). The RFI problem in Juneau occurs frequently since two of the profilers are in a direct line of sight with each other. NIMA has the capability of identifying and tracking RFI in time (see Morse et al. 2002). NIMA rarely selects RFI instead of an atmospheric signal unless the atmospheric signal is near to the RFI in the given beam. NIMA rejects point targets and rarely selects ground clutter unless the ground clutter is located near the atmospheric signal. Some additional data from a larger 9-month database were also analyzed. These were cases where the NWCA winds had large temporal discontinuities, and contained low SNR cases where NIMA generated incorrect first moments. In addition, the verification database contained data from the South Douglas Island profiler where a beam-switching problem made the wind estimates unreliable. These data and the additional data from the 9-month database were included in the study as a test of the NWCA wind confidence algorithm. This database was chosen to include very challenging data scenarios, and hence some of these data are not typical of profiler data collected in Juneau.

Human verification was done on the Doppler moments in the database. A graphical interface was available to the human experts performing the verification (see Cohn 2001 for a description of the methodology used in this verification effort.) Using this interface, the human experts chose the location of the atmospheric signal, which was then used to compute the moments. The experts also estimated a confidence for each of these moments. The error in a first moment is defined as the difference between the human first moment estimate and the NIMA first moment estimate. Here we are assuming the human estimate to be truth. The absolute error is defined as the absolute value of the error. There were wind profiles containing over 6000 first moment estimates in the database provided by human verification. The average absolute error was 0.49 m s^{-1} with a root-mean-Square (rms) error of 1.32 m s^{-1}. This rather large rms indicates the presence of outliers. Most of these outliers are caused by low SNR cases as well as some cases where NIMA selected ground clutter as part of the atmospheric signal. When the first moment estimates with the lowest 20% of NIMA-calculated confidence are removed, the average absolute error was approximately 0.3 m s^{-1}, which is the spectral resolution of the profilers used in Juneau. The rms was reduced to slightly less than 1 m s^{-1}. This indicates that NIMA first moment confidence has skill in reducing first moment outliers and errors.

NIMA first moment confidence is a factor in computing NWCA wind confidence (see section 4). Although NIMA first moment confidence has skill in identifying outliers, it can, in rare circumstances, give outliers high confidence (Cohn et al. 2001). In fact, outliers in the first moment measurements will often violate many of the assumptions made in computing the horizontal wind (section 2) and should result in a lower wind confidence (see the discussion in section 4). The NWCA wind confidence should have skill in removing additional outliers that were given a high NIMA first moment confidence.

As part of the verification exercise, the profiles were verified in groups of four (north, south, east, and west beams). A human-verified wind was produced using Eqs. (12) and (13) where the a_E, a_W, a_N, and a_S values are the human-verified first moments. The NWCA error is defined as the difference between the human-verified horizontal wind components and the NWCA horizontal wind components. The NWCA absolute wind error is defined as the square root of the sum of the squares of these errors. The NWCA wind speed error is the difference between the human-verified wind speed and the NWCA-produced wind speed. The absolute error in the wind speed is the absolute value of wind speed error. The verification dataset contains over 2400 human-verified horizontal wind components.

In order to make a further comparison, POP [Profiler On-line Program, Carter et al. (1995)] were also compared to human-verified wind speeds. This algorithm is based on locating the peak intensity of the signal at each range gate and following that signal to the noise floor. The signal thus collected is used to calculate the POP first moment. This algorithm produces high-quality first moments for uncontaminated spectra. However, when contaminants have spectral intensities greater than that of the atmospheric signal, erroneous moments are often generated (Morse et al. 2002). In traditional profiler applications such erroneous moments are not particularly problematic as they are eliminated through consensus averaging over time periods of 30 min or more. Rapid update winds are required in the airport hazard application described in the introduction. The POP algorithm returns first moment estimates approximately every 30 s, and these may be used to compute rapid update winds similar to the way human-verified first moments are used to produce horizontal winds. It is these rapid update winds from POP moments that are compared to the human-verified horizontal winds. Figure 2 shows a scatterplot comparing the rapid update POP wind speeds to the human-verified wind speeds in meters per second. Notice the large number of outliers that give an rms of 9.9 m s^{-1} and an average absolute error of 4.7 m s^{-1}. These outliers are caused by several factors including RFI, ground clutter, point targets, and low SNR. In addition, the beam-switching problem at South Douglas Island produced unreliable winds. The South Douglas Island profiler is located in the Gasteneau Channel

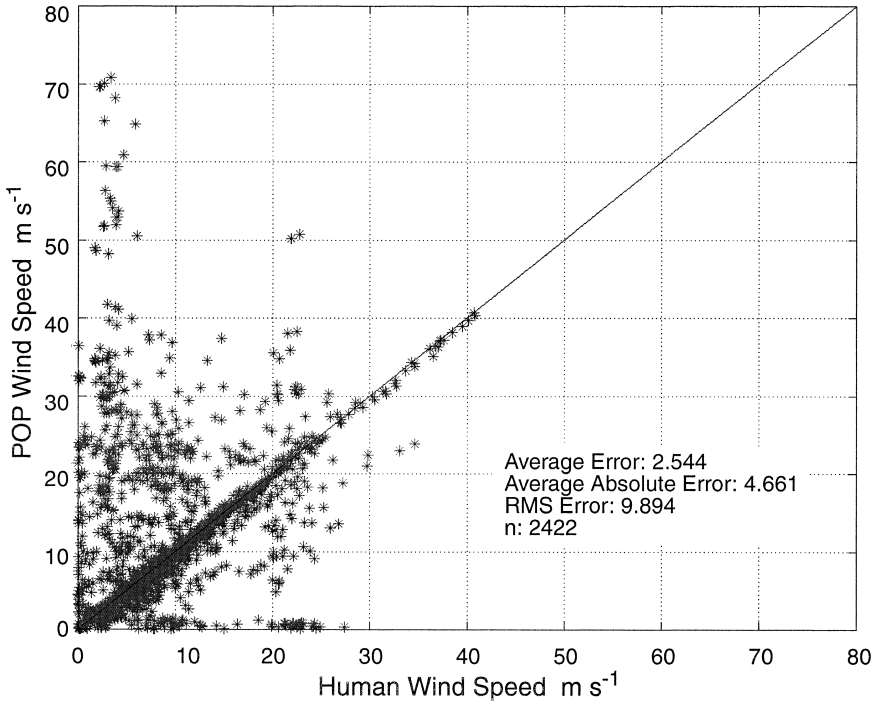

FIG. 2. A scatterplot comparing the human-verified wind speed in m s^{-1} (horizontal or x axis) and the POP wind speeds in m s^{-1} (vertical or y axis). The line $y = x$ line is shown for reference. Notice the large number of outliers.

where the winds are often dry and have a low SNR. If we remove the South Douglas Island data (about 35% of the data), Fig. 3 shows a definite improvement. The rms is now 6.7 m s^{-1} and the average absolute error in the wind speed has been reduced to 3.4 m s^{-1}. The data in Fig. 3 does not contain the beam-switching problem, but the two remaining profilers have a significant RFI problem since they are in direct line of sight of each other.

Figure 4 shows a scatterplot of NWCA wind speeds in comparison to human-verified wind speeds. Notice there are significant outliers, but many fewer outliers than in the POP analysis. The average absolute error is 1.8 m s^{-1} and an rms of 4.4 m s^{-1}. These statistics are an improvement over the POP analysis even when the South Douglas Island data were removed from the POP analysis in Fig. 3.

Figure 5 shows the same data as Fig. 4 except the South Douglas Island data have been removed. Now the average absolute error in the wind speed is 0.9 m s^{-1} with an rms of 1.6 m s^{-1}. This shows that many of the outliers have been removed, but there remains a cluster of outliers at (20,10) in Fig. 5. Comparing Figs. 2 and 3 to Figs. 4 and 5, it is clear that rapid update NWCA wind speeds compare better to human-verified wind speeds than those produced by the peak-finding algorithm. This is because NIMA produces first moments that are less prone to RFI, point targets, and ground clutter contamination. The peak-finding algorithm produces better results when SNR is used as a confidence value. However, to obtain an average absolute error in first moment estimates of 0.3 m s^{-1}, 60% of the data with the lowest SNR must be removed. In contrast, this level of performance is obtained for NIMA first moments when the lowest 20% of first moment data is removed as measured by the first moment confidence algorithm.

With these results as a baseline, a study of the wind confidence algorithms is provided. By removing the South Douglas Island data profiler from the analysis, the human-estimated wind speeds were in better agreement with the NWCA wind speeds. Since there were problems in the South Douglas Island wind data due to the beam-switching problem, much of the data should be classified as poor quality data by the wind confidence algorithm. To test this proposition, about 30% of the data as classified by low wind confidence were removed from the dataset (this corresponds to removing all data below the threshold of 0.56 wind confidence). Figure 6 shows a scatterplot of the resulting data compared to the human-estimated wind speeds. Notice that the average absolute error is now 0.74 m s^{-1} and has an rms of 1.26 m s^{-1}. The cluster of outliers at (10, 20) remains, but the number of points has been reduced from 12 to 3 points. Thus many of the poor quality South Douglas Island data were removed by the wind confidence algorithm, and additional outliers in the remaining data were also removed. This is because some of the South

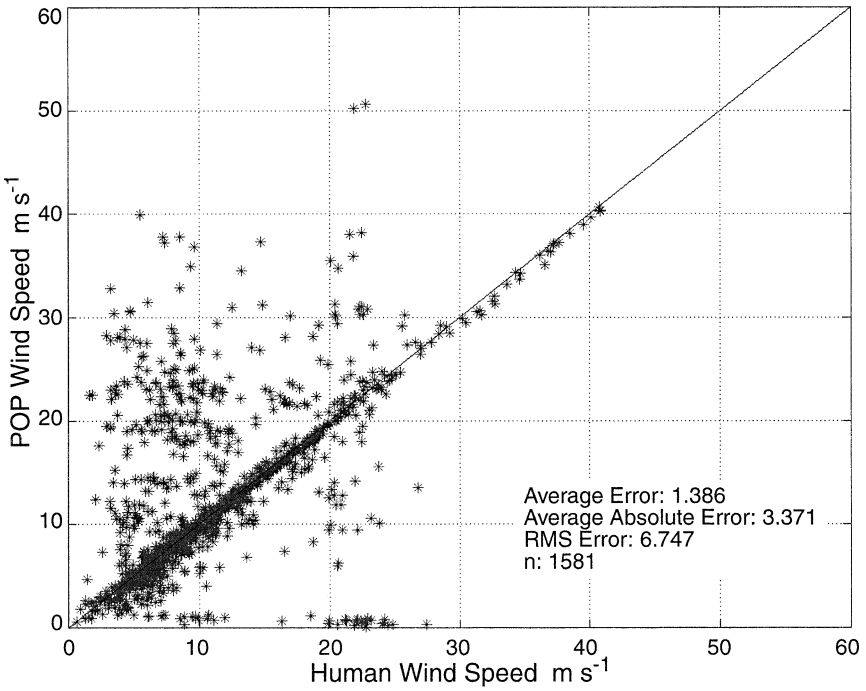

FIG. 3. The same as Fig. 2 except that the South Douglas Island data have been removed. Notice the improved statistics in the upper-left corner of the scatterplot. The remaining outliers are due to point targets, low SNR, ground clutter, and RFI.

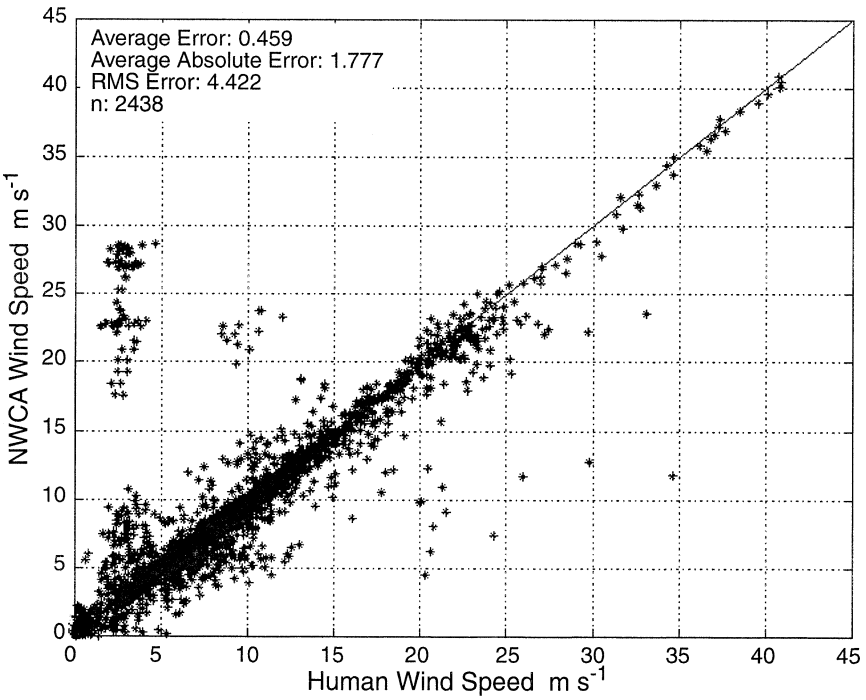

FIG. 4. A scatterplot similar to Fig. 2 comparing the human-verified wind speed to the NWCA wind speed. The large outliers on the left of the figure are due to the beam-switching problem at South Douglas Island.

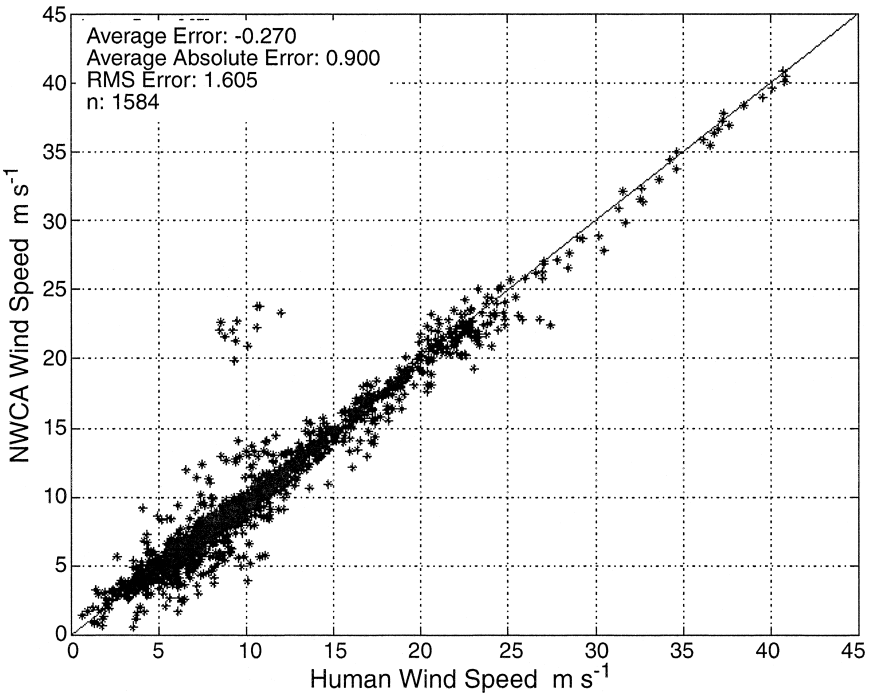

FIG. 5. The same as Fig. 4 except the South Douglas Island data have been removed. The cluster of outliers at around (10,20) are due to low SNR cases.

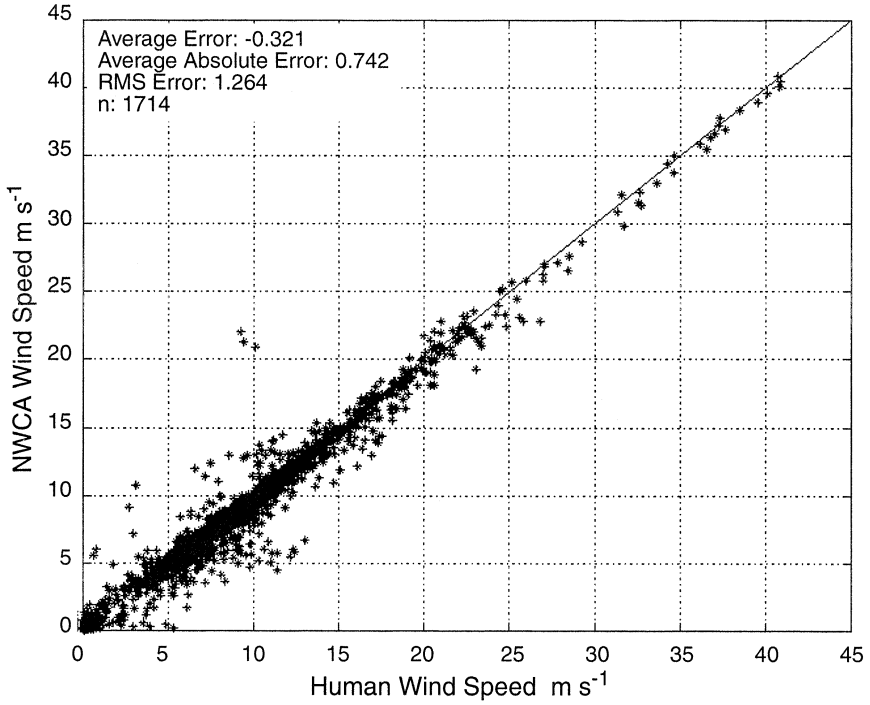

FIG. 6. The same as Fig. 4 except that the data with the lowest 30% wind confidence values have been removed. Notice that the size of the cluster of outliers around (10,20) has been reduced when compared with Fig. 5. The cluster of outliers at the left in Fig. 4 have also been removed. Notice also the improved statistics compared to Figs. 4 and 5.

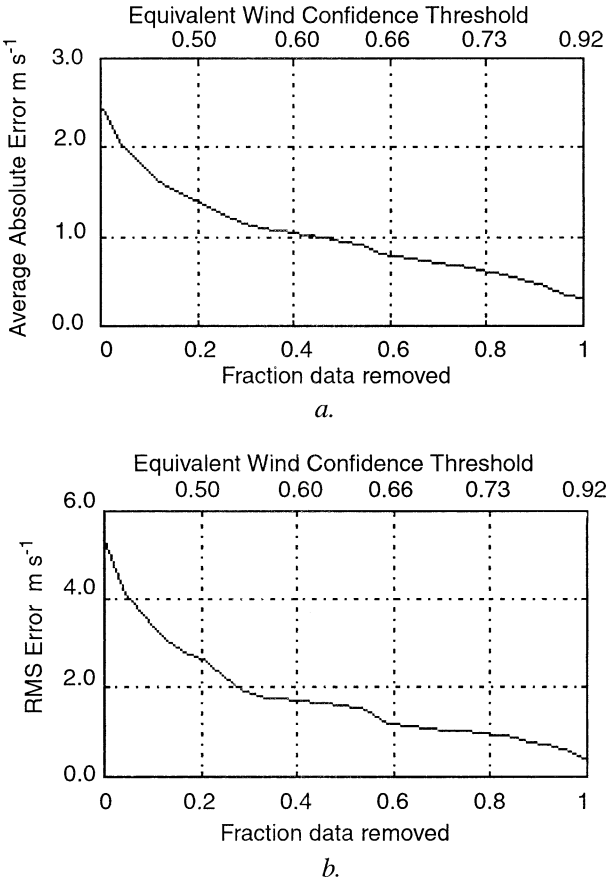

FIG. 7. (a) A graph of the average absolute error (average length of the remaining error vectors) in m s^{-1} (vertical axis) as a function of the percentage of data removed (lower horizontal axis). The upper horizontal axis is the corresponding wind confidence threshold. When all data with wind confidence less than 0.6 have been removed, 40% of the data has been removed, and the average absolute error is about 1 m s^{-1}. (b) A graph of the rms of the length of the remaining error vectors (vertical axis) as a function of the percentage of data removed. This is an indicator of outliers. Notice the curve decreases with increasing wind confidence.

Douglas Island data did not satisfy the wind assumptions (discussed in section 2) because of the switching error, and subsequently had low confidences based on the application of the tests described in section 4. In fact, this switching problem was discovered because the South Douglas profiler reported persistent low confidence winds. Additional first moment outliers are detected because the resulting winds do not satisfy the tests described in section 4, and hence the resulting winds have low wind confidence. The NWCA wind speed error indicators such as absolute error and rms error continue to decrease as the wind confidence threshold is increased. To see this in a different way, the average absolute error in the horizontal components (viewed as a two-dimensional vector) as a function of the amount of data removed as ranked by NWCA wind confidence is examined.

Figure 7a shows the average absolute vector error as a function of the data removed. The vertical axis in the absolute vector error, and the lower horizontal axis, is the percent of data removed. Thus when the data with the lowest 40% of NWCA confidence have been removed, the average absolute vector error is about 1 m s^{-1}. The upper horizontal axis is the equivalent NWCA confidence threshold. Thus when all data with a wind confidence less than 0.6 are removed, 40% of the data have been removed. Figure 7b shows the rms as a function of percent of data removed. Notice both curves in Fig. 7 continue to decrease as the quality of the data improves, where the quality of the data is measured by the wind confidence. The absolute vector error as measured by the length of the error vector is a strict test. By the triangle inequality, the absolute vector error dominates the absolute error in wind speed. Figure 7 shows that the wind confidence algorithm may be used to ensure high-quality wind estimates.

As mentioned above, the evaluation dataset is not representative of the data in Juneau. The average wind confidence for the 9-month period of 18 November 1998–31 July 1999 was 0.78 compared to the average value of 0.66 for the verification dataset. This 9-month period did not contain the beam-switching problem at the South Douglas Island profiler. However, the winter months are of interest since this is the period of high turbulence in Juneau. Data for the period of 7 December 1999–14 February 2000 were analyzed. Figure 8a shows an estimate of the probability distribution function for wind confidences. The mean is 0.68, which is close to the value of 0.66 for the verification dataset. An estimate for the cumulative distribution function for the wind confidences is shown in Fig. 8b. This dataset did not contain the South Douglas Island beam-switching problem. Notice that to remove all data with a threshold less that 0.557 requires the removal of only about 18% of the data. Assuming performance is similar for this dataset as for the verification data, this implies that the horizontal wind vector estimate has an average vector error of about 1 m s^{-1} and an average absolute error in the wind speed of 0.74 m s^{-1} after 18% of the data is removed. During other times of the year, even fewer data need to be removed to obtain this level of performance. In the 9-month database, the confidence of the confidence-weighted average wind was less than 0.56 only 3% of the time. These fractions are representative of this Juneau data only and should not be extrapolated to other sites or profiler operating parameters. For example, if measurements were routinely made at heights much greater than 2.5 km where the signal strength is less, a larger fraction of measurements would be removed by the confidence threshold of 0.557 seemingly needed to achieve an average error of 1 m s^{-1}.

7. Conclusions

An analysis describing the estimation of linear wind field parameters in a four- or five-fixed-beam profiler

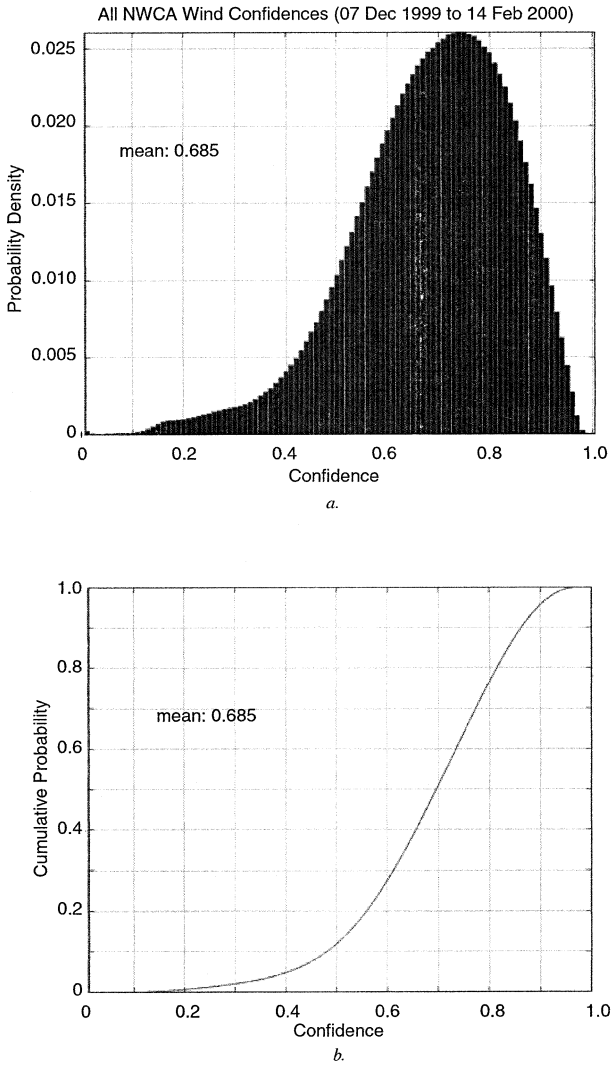

FIG. 8. (a) The probability density function of the NWCA wind confidence for all three profilers during the time period 7 Dec 1999–14 Feb 2000. (b) The cumulative distribution function of the probability density function in (a). Notice that the data have about 12% of the data with wind confidence below 0.5.

system has been presented. It has been shown that it is possible to estimate the horizontal components of the wind in a reliable way with a typical profiler geometry under the assumptions that the wind is modeled by a linear wind field, that the vertical wind component is constant in the horizontal directions, and that the wind is stationary over the sampling region. It has also been established that it is possible to give reasonable estimates for the vertical shear of the horizontal components of the wind. When the assumptions upon which the analysis is based break down, confidence indices are available that can be used both to identify the wind estimates as unreliable and to remove outliers in the wind estimates. A description of these wind confidence indices and how they are derived based on testing the validity of those assumptions has been given. These confidence indices are also used to generate a confidence-weighted average wind value. The performance of the NWCA algorithm was discussed and it was shown that the confidence indices show skill in reducing first moment and wind estimate errors, based on ''truth'' values available from human expert analysis.

The NWCA algorithm has been running in near real time in Juneau, Alaska, since February 1998. Modifications continue and it is expected that this algorithm will eventually be an integral part of a turbulence and shear warning system for the Juneau airport.

Acknowledgments. This research is in response to requirements and funding by the Federal Aviation Administration (FAA). The views expressed are those of the authors and do not necessarily represent the official policy or position of the FAA.

APPENDIX

Measurement Error Effects on Wind and Shear Estimates

In the main discussion, it was assumed that measurements were made without error. However, it is important to account for the effect of measurement errors on the wind and shear estimates derived from these measurements. To account for these errors, Eq. (1) is modified to

$$\mathbf{V}(\mathbf{x}) = \mathbf{V}(\mathbf{x}_o) + \mathbf{A} \cdot (\mathbf{x} - \mathbf{x}_o) + \boldsymbol{\varepsilon} \qquad \text{(A1)}$$

where

$$\boldsymbol{\varepsilon} = \begin{bmatrix} \varepsilon_x \\ \varepsilon_y \\ \varepsilon_z \end{bmatrix}.$$

The terms ε_x, ε_y, ε_z are assumed to be independent with expected values of zero and each with the same variance σ^2. Furthermore, it is assumed that these errors are homogeneous in space and stationary in time. In the case of atmospheric turbulence these error terms along a radial will not be independent. To study this, a model of the autocovariance function is required. This depends on the particular model of turbulence studied. Equation (5.3.5) in Priestley (1981) shows the variance as a function of the autocovariance function. The more correlated the data, the more averaging that is required to reduce the variance. It is beyond the scope of the present paper to include this type of analysis. For the case of small measurement errors, it is reasonable to assume independence. In order to compare our results to a statistical analysis, the first moment confidences are all assumed to be equal as well.

Along a radial defined by the unit vector $\mathbf{e} = [\sin\phi \cos\theta, \sin\phi \sin\theta, \cos\phi]^T$, the radial velocity becomes $V_r = \mathbf{V}(\mathbf{x}) \cdot \mathbf{e} = \mathbf{V}(\mathbf{x}_o) \cdot \mathbf{e} + A \cdot (\mathbf{x} - \mathbf{x}_o) \cdot \mathbf{e} + \varepsilon \cdot \mathbf{e}$. Analogously to Eq. (3), the radial velocity can be modeled as

$$V_r = a + b(r - r_0) + \varepsilon_r,$$

(A2)

where the error term ε_r is given by

$$\varepsilon_r = \boldsymbol{\varepsilon} \cdot \mathbf{e} = \varepsilon_x \sin\phi \cos\theta + \varepsilon_y \sin\phi \sin\theta + \varepsilon_z \cos\phi. \quad \text{(A3)}$$

From Eq. (A3) it follows that the expected value $E(\varepsilon_r) = 0$, and the variance $\mathrm{Var}(\varepsilon_r) = \sigma^2$, and holds for any given radial. This follows from the fact that $\mathrm{Var}(\Sigma_i a_i \varepsilon_i) = \Sigma_i a_i^2 \mathrm{Var}(\varepsilon_i)$ if the ε_i are independent, and $E(\Sigma_i \varepsilon_i) = \Sigma_i E(\varepsilon_i)$.

The radial velocity V_{r_i} is sampled at the points $r_i = r_0 + i\Delta r$ along the radial, where $i = -N, \ldots, -1, 0, 1, \ldots, N$, and a and b are estimated by $\hat{a}$ and $\hat{b}$, where $\hat{a}$ and $\hat{b}$ are chosen to minimize

$$R^2 = \sum_{-N}^{N} [V_{r_i} - (\hat{a} + \hat{b} i\Delta r)]^2 c_i, \quad \text{(A4)}$$

where R is the residual between the data and the model.In Eq. (A4), the confidences (here weights in the minimization process) c_i are assumed to be equal and nonzero. Taking the partial derivatives of R^2 with respect to $\hat{a}$ and $\hat{b}$, and setting these equal to zero, $\hat{a}$ and $\hat{b}$ are given by

$$\hat{a} = \frac{\sum_{-N}^{N} V_{r_i}}{2N+1} \qquad \hat{b} = \frac{\sum_{-N}^{N} i V_{r_i}}{\frac{N(2N+1)(N+1)}{3}\Delta r}. \quad \text{(A5)}$$

Substituting Eq. (A2) into Eq. (A5), gives the standard result:

$$\hat{a} = a + \frac{\sum_{-N}^{N} \varepsilon_{r_i}}{2N+1},$$

$$\hat{b} = b + \frac{\sum_{-N}^{N} i\varepsilon_{r_i}}{\frac{N(2N+1)(N+1)}{3}\Delta r}. \quad \text{(A6)}$$

Let

$$\varepsilon_r' = \frac{\sum_{-N}^{N} i\varepsilon_{r_i}}{\frac{N(2N+1)(N+1)}{3}\Delta r}.$$

From Eq. (A6) and the remark following Eq. (A2), it can be seen that $\hat{a}$ is an unbiased estimator of a with variance $\sigma^2/(2N+1)$. Also $\hat{b}$ is an unbiased estimator of b with variance

$$(\sigma')^2 = \frac{\sigma^2}{\frac{N(2N+1)(N+1)}{3}(\Delta r)^2}.$$

These results hold for any radial.

Applying this result to Eqs. (7) and (10) yields

$$\hat{a}_E - \hat{a}_W = a_E - a_W + \varepsilon_E - \varepsilon_W = 2u_V \sin\phi + 2w_x r_0 \sin\phi \cos\phi + \varepsilon_E - \varepsilon_W.$$

Therefore an estimate for u_V is

$$\hat{u}_V = \frac{\hat{a}_E - \hat{a}_W}{2\sin\phi} = u_V + w_x r_0 \cos\phi + \frac{\varepsilon_E - \varepsilon_W}{2\sin\phi}. \quad \text{(A7)}$$

Thus the estimate $\hat{u}_V$ for u_V is a biased estimate with bias $w_x r_0 \cos\phi$ and variance $\sigma^2/[2(2N+1)\sin^2\phi]$. In the case where $w_x = 0$, $\hat{u}_V$ is an unbiased estimator for u_V. In a typical application, $N = 2$ and $\phi = 15°$, so that the variance is about $1.5\sigma^2$. A similar result holds for v_V. In Cohn et al. (2001) it is established that after the data with lowest 25% NIMA first moment confidence is removed, there is a measurement error of $\sigma = 0.6$ m s^{-1} when comparing NIMA first moments to human estimates. If this value for σ is used, a variance of 0.54 m^2 s^{-2} results.

Next consider estimates for the various shears. Substituting into Eq. (20) the estimates for u_x yield

$$\begin{aligned}\hat{u}_x &= \frac{\hat{b}_E + \hat{b}_W}{2\sin^2\phi} - \hat{w}_z \frac{\cos^2\phi}{\sin^2\phi} \\ &= \frac{b_E + b_W + \varepsilon_E' + \varepsilon_W'}{2\sin^2\phi} - (w_z + \varepsilon_V')\frac{\cos^2\phi}{\sin^2\phi} \\ &= \frac{b_E + b_W}{2\sin^2\phi} - w_z \frac{\cos^2\phi}{\sin^2\phi} + \frac{\varepsilon_E' + \varepsilon_W'}{2\sin^2\phi} - \varepsilon_V' \frac{\cos^2\phi}{\sin^2\phi} \\ &= u_x + \frac{\varepsilon_E' + \varepsilon_W'}{2\sin^2\phi} - \varepsilon_V' \frac{\cos^2\phi}{\sin^2\phi},\end{aligned}$$

where ε_V' is the error term for the vertical radial when computing w_z. Thus $\hat{u}_x$ is an unbiased estimator for u_x with variance

$$\mathrm{Var}(\hat{u}_x) = \frac{2(\sigma')^2}{4\sin^4\phi} + (\sigma')^2 \frac{\cos^4\phi}{\sin^4\phi} = \frac{3\sigma^2}{N(2N+1)(N+1)(\Delta r)^2 \sin^4\phi}\left(\frac{1}{2} + \cos^4\phi\right). \quad \text{(A8)}$$

In a typical application, that is, $N = 2$, $\phi = 15°$, $\Delta r = 60$ m, the resulting variance is about $0.0085\sigma^2$. If again the value of $\sigma = 0.6$ m s^{-1} is used, a variance of 0.003 s^{-2} results. This represents a large shear, $[\mathrm{Var}(\hat{u}_x)]^{1/2} = 0.05$ s^{-1}. This shows why it is difficult to estimate u_x without averaging over a large amount of time. Thus only persistent shears in u_x can be found. At present in the Juneau system, there is no attempt to estimate u_x. To estimate u_x a vertical beam would be required and some time averaging would be required to further reduce this variance.

Consider estimating u_z, again by applying Eq. (20) to yield

$$\hat{u}_z + \hat{w}_x = \frac{\hat{b}_E - \hat{b}_W}{2\sin\phi\cos\phi} = \frac{b_E - b_W + \varepsilon'_E - \varepsilon'_W}{2\sin\phi\cos\phi}$$

$$= u_z + w_x + \frac{\varepsilon'_E - \varepsilon'_W}{2\sin\phi\cos\phi}.$$

Thus $(\hat{b}_E - \hat{b}_W)/(2\sin\phi\cos\phi)$ is a biased estimate for u_z with bias w_x and variance

$$\mathrm{Var}(\hat{u}_z) = \frac{(\sigma')^2}{2\cos^2\phi\sin^2\phi}$$

$$= \frac{3\sigma^2}{2N(2N+1)(N+1)\cos^2\phi\sin^2\phi(\Delta r)^2}$$

$$= 0.000\,222\sigma^2,$$

using the same parameters as in the calculation of $\mathrm{Var}(\hat{u}_x)$. This will be an unbiased estimate assuming $w_x = 0$. With $\sigma = 0.6$ m s^{-1}, this becomes $\mathrm{Var}(\hat{u}_z) = 0.000008$ s^{-2} and $[\mathrm{Var}(\hat{u}_z)]^{1/2} = 0.0089$ s^{-1}. This is more than an order of magnitude smaller than the variance for finding u_x. With some time or spatial averaging it should then be possible to measure u_z and v_z for persistent shears. Such shears have been detected in Juneau and they are often associated with strong turbulence.

REFERENCES

Abraham, B., and J. Ledolter, 1983: *Statistical Methods for Forecasting.* Wiley, 445 pp.

Boccippio, D. J., 1995: A diagnostic analysis of the VVP single-Doppler retrieval technique. *J. Atmos. Oceanic Technol.,* **12,** 230–248.

Browning, K. A., and R. Wexler, 1968: The determination of kinematic properties of a wind field using Doppler radar. *J. Appl. Meteor.,* **7,** 105–113.

Carter, D. A., K. S. Cage, W. L. Ecklund, W. M. Angevine, P. E. Johnston, A. C. Riddle, J. Wilson, and C. R. Williams, 1995: Developments in UHF lower tropospheric wind profiling at NOAA's Aeronomy Laboratory. *Radio Sci.,* **30,** 977.

Cohn, S. A., R. K. Goodrich, C. S. Morse, E. Karplus, S. Mueller, L. B. Cornman, and R. A. Weekley, 2001: Radial velocity and wind measurement with NIMA: Comparisons with human estimation and aircraft measurements. *J. Appl. Meteor.,* **40,** 704–719.

Cornman, L. B., R. K. Goodrich, C. S. Morse, and W. L. Ecklund, 1998: A fuzzy logic method for improved moment estimation from Doppler spectra. *J. Atmos. Oceanic Technol.,* **15,** 1287–1305.

Forsythe, G. E., M. A. Malcolm, and C. B. Moler, 1977: *Computer Methods for Mathematical Computations.* Prentice Hall, 249 pp.

Freund, J. E., 1992: *Mathematical Statistics.* 5th ed. Prentice Hall, 658 pp.

Koscielny, A. J., R. J. Doviak, and D. S. Zrnić, 1984: An evaluation of the accuracy of some radar wind profiling techniques. *J. Atmos. Oceanic Technol.,* **1,** 309–320.

Morse, C. S., R. K. Goodrich, and L. B. Cornman, 2002: The NIMA method for improved moment estimation from Doppler spectra. *J. Atmos. Oceanic Technol.,* **19,** 274–295.

Press, W. H., B. P. Flannery, S. A. Tenkolsky, and W. T. Vetterling, 1988: *Numerical Recipes in C.* Cambridge University Press, 735 pp.

Priestley, M. B., 1981: *Spectral Analysis and Time Series.* Academic Press, 890 pp.

Strauch, R. G., D. A. Merritt, K. P. Moran, K. B. Earnshaw, and D. van de Kamp, 1984: The Colorado wind-profiling network. *J. Atmos. Oceanic Technol.,* **1,** 37–49.

——, B. L. Weber, A. S. Frisch, C. G. Little, D. A. Merritt, K. P. Moran, and D. C. Welsh, 1987: The precision and relative accuracy of profiler wind measurements. *J. Atmos. Oceanic Technol.,* **4,** 563–571.

Waldteufel, P., and H. Corbin, 1979: On the analysis of single-Doppler radar data. *J. Appl. Meteor.,* **18,** 532–542.